Available online at www.sciencedirect.com
ScienceDirect
Journal of Nuclear Materials 367–370 (2007) 599–602
journal of nuclear materials
www.elsevier.com/locate/jnucmat

Small fracture toughness specimen for post-irradiation experiments

H.-C. Schneider *, J. Aktaa, R. Rolli

Forschungszentrum Karlsruhe GmbH, Institute for Materials Research, P.O. Box 3640, D-76021 Karlsruhe, Germany

Abstract

A subsized specimen for fracture-mechanics tests as well as the associated test devices have been developed and applied to examinations of ferritic–martensitic steels in irradiated and unirradiated conditions. Non-conservative results are prevented by geometrical modification of the fracture zone and appropriate test and evaluation techniques. Experimental and computational comparison to standard samples is presented. The shift in ductile-to-brittle transition of the fracture toughness – compared to full-scale specimens – is examined in experiments at different temperatures. Evaluation of samples irradiated to 0.8 dpa at temperatures between 250 and 450 °C provides reproducible values for J and K and allows complete J–R-curves to be derived. Fracture toughness in the upper shelf is strongly reduced by up to 60% by irradiation, and the ductile-to-brittle transition temperature is raised to 140 °C.

1. Introduction

A broader data base of irradiated fracture toughness results is needed for fusion reactor materials. The size limitations of irradiation programs require small specimens, post-irradiation examination necessitates a geometry which is insensitive to remote handling, and the standards of fracture toughness tests include minimum size requirements and geometric restrictions. Many theoretical and experimental work has been accomplished on the topic of small fracture-mechanics specimens, e.g. the overview given by Odette et al. [1], the experiments performed by Wallin et al. [2] and the numerical evaluations of Nevalainen and Dodds [3]. In the present work, a $9 \times 18\ \mathrm{mm}^2$ three-point-bending specimen is in a first step reduced in size to $3 \times 6\ \mathrm{mm}^2$ without changing the geometry. In a second step, the geometry is changed towards $3 \times 4\ \mathrm{mm}^2$, keeping the ligament constant. This allows a separate identification of pure size- and geometrical effects.

1.1. Specimen geometry, test and evaluation procedure

The specimen is based on the KLST-type Charpy specimen, suitable for irradiation programs under limited space conditions (Fig. 1) and can be inserted in irradiation rigs with KLST specimens. It is

* Corresponding author. Address: Forschungszentrum Karlsruhe, Institute for Materials Research II, Hermann-von-Helmholtz-Platz 1, D-76344 Eggenstein-Leopoldshafen, Germany. Tel.: +49 0721 82 4568; fax: +49 0721 82 5882.
E-mail address: hans-christian.schneider@imf.fzk.de (H.-C. Schneider).

0022-3115/$ - see front matter © 2007 Elsevier B.V. All rights reserved.
doi:10.1016/j.jnucmat.2007.03.104

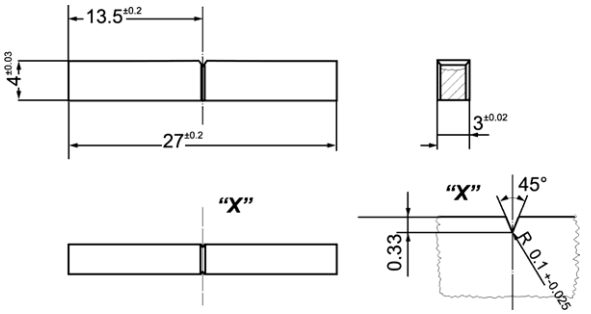

Fig. 1. Subsized fracture-mechanics specimen (side-grooved). $W = 4$ mm, $B = 3$ mm, a (crack length) = 1 mm.

grooved for 0.5 mm and precracked by a resonance bending machine for another 0.5 mm, which leads to a ligament length, $W - a$, of 3 mm and a relation of $a/W = 0.25$. This is different from the standard recommendation of 0.5. Where the ductile material state requires it, the specimen is side-grooved (0.33 mm) after the precracking procedure.

A universal testing machine with 3-point-bending equipment was used for quasi-static tests, and instrumented pendula (25*J*) for unirradiated and irradiated dynamic tests. Two different evaluation methods were employed for the dynamic tests. Schindler and Tipping give a relation to obtain a complete J–Δa-curve by evaluation of the force-vs.-deflection curve of the instrumented test [4]. Therefore, C and p parameters are calculated from the impact energy at the point of maximum force, E_m, the total energy, and the initial crack length a.

$$J(\Delta a) = C \cdot \Delta a^p. \tag{1}$$

J_{ID}, can also be calculated directly using a relation given by Zhang and Shi [5]. Here, the characteristic energy, $(E_m)_r$, at the onset of fracture propagation is calculated by the maximum force, the time to onset of plastic deformation, and the compliance.

$$J_{ID} = \frac{2(E_m)_r}{B_n(W - a_0)}. \tag{2}$$

1.2. Calculation of J-distribution

Correct determination of K_{IC} and J_{IC} requires a two-dimensional strain-state in the fracture zone. Near the surface of the specimen, it is three-dimensional and leads to fracture along the main shear stress instead of separation in mode-I direction. This area of shear fracture becomes more important with decreasing specimen size. It leads to overestimating the material toughness, as the critical force or energy is higher than for pure mode-I fracture.

Three-dimensional finite-element calculations of the different geometries were performed modelling quarters of specimen using their planes of symmetry, employing 8-nodal elements with eight integration points (Abaqus V6.2 element types C3D8 and C3D8H). The stress distribution was calculated at the crack tip, and *J*-Integrals were obtained by contour-integrals applying virtual crack extension. Material parameters were derived from instrumented tensile experiments of all materials and material states investigated in fracture-mechanics experiments.

Evaluation of different variations of side-grooves lead to the geometry indicated in Fig. 1. The stress state in front of the crack tip is uniformly distributed for a wide range due to artificial constraints. Fig. 2 illustrates the different distribution of the *J*-Integral in the fracture zone of a plane-sided specimen and a specimen according to Fig. 1, both with ductile material behaviour of EUROFER 97 at room temperature. For the plane specimen, the distribution of J follows the stress distribution in the mode-I direction; it is strongly reduced near the surface. There is a huge difference between the maximum J_{max} (which can be considered as dominant for the local crack extension) and the average J_{avg} (which can be compared to J determined experimentally). For the specimen with lateral notches, the *J*-distribution is clearly homogeneous (despite the direct vicinity of the notch root). The difference between J_{max} and J_{avg} is reduced by 75% in comparison to the plane specimen.

2. Experiments

Isothermal experiments are performed at room temperature (*RT*) in three different material condi-

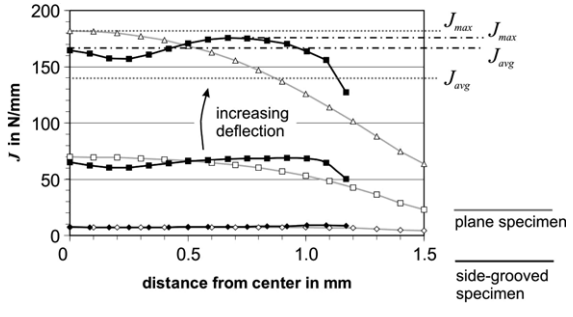

Fig. 2. Distribution of the *J*-integral in plane (grey) and side-grooved (black) specimens for different deflections.

tions; in ductile, and in brittle condition, and in the transition region between both of them. Different specimen sizes, geometries, and materials were used (Tables 1 and 2). For brittle material, K_{IC} can be determined according to the ASTM E 399 standard, apart from the size criteria. Plane full-sized and subsized specimens lead to results in the range of 62–72 MPa $m^{0.5}$; lateral grooves are not necessary. If they are applied nevertheless, they do not influence the result in a decisive manner.

In the ductile regime, no direct determination of K_{IC} is possible. J_{IC} allows the determination of the stress intensity K_{JIC} which can be used for comparison with the K_{IC}-results obtained in brittle conditions. Table 3 shows J_{IC} and K_{JIC} determined by the multi-specimen method via the J_t-determination for different types of specimens. The crack opening displacement is determined directly for all specimens, as it was found that the blunting line overestimates it in a relevant manner. For all specimens, maximum crack opening displacement was found at approximately only 0.1 mm; the resulting J_{IC}-values were reasonably lower then for the blunting line method. A determination of $J_{0.2}$ also was done and revealed the same J_{IC}, if the local values of J and crack propagation were respected in a similar manner to the m-factor presented for different specimen geometries by Nevalainen and Dodds [3].

Table 1
Steels investigated, chemical composition in wt%

	EUROF.97	MANET-I	MANET-II
T_{aust} (°C)	1040	1075	1075
T_{tmp} (°C)	760	700	600/700
Cr	8.91	10.8	9.94
W	1.08		
Mn	0.48	0.76	0.79
N	0.02	0.02	0.023
Ta	0.14		
C	0.12	0.14	0.1
V	0.2	0.2	0.22
B	0.001	0.0085	0.007
Ti	0.006		
Fe	Balance	Balance	Balance

Table 2
Direct determination of K_{IC} (MANET-II, brittle)

B (mm)	a/W (–)	K_{IC} (MPa $m^{0.5}$)
9, Plane	0.5	68–76 (avg. 72)
3, Plane	0.5	58–65 (avg. 62)
3, Side-grooved	0.5	63–73 (avg. 68)
3, Plane	0.25	67–70 (avg. 68)
3, Side-grooved	0.25	59–61 (avg. 60)

Table 3
Determination of J_{IC} and of K_{JIC} via J_{IC} (EUROFER 97, ductile)

B (mm)	J_{IC} (N/mm)	K_{JIC} (MPa $m^{0.5}$)
9, Plane	288	258
9, Side-grooved	283	256
3, Plane	316	270
3, Side-grooved	277	253

Full-sized specimens yield the same results with and without side-grooving; whereas plane subsized specimens reveal higher toughness values. Side-grooves as mentioned above reduce the toughness to the levels of the full-size specimens. For all specimen sizes and geometries, EUROFER 97 shows clearly better results than the preceding structure material candidate alloys MANET-I and -II, both in absolute values and in the ductile-to-brittle-transition temperature.

In the transition regime, results for different specimen sizes differ clearly at RT (Table 4). Full-sized specimens indicate a much lower toughness. Caused by the constraint loss in small specimens, the fracture-mechanics ductile-to-brittle transition temperature, $DBTT_{JID}$, decreases below RT with the specimen size. $DBTT_{JID}$ here is determined at 50% of upper shelf value of J_{ID}, the same way as transition temperature in the Charpy tests, $DBTT_{USE}$, is determined at 50% of the upper shelf energy. The systematic size-dependent difference in $DBTT_{USE}$ was documented for variations of 10 and 3 mm wide specimens by Kaspar and Faul [6]. Analogous differences are shown in Table 4 as well for Charpy- as for fracture toughness tests of MANET-II (for two different tempering temperatures). Size reduction reduces $DBTT_{USE}$ by 50 °C; for fracture toughness tests, the same reduction can be observed at a level approximately 40 °C higher. Detailed results of all experiments can be found in [7]. For these investigations, no significant difference for the specimens with $a/W = 0.5$ or 0.25 can be found.

Table 4
Determination of J_{IC} (MANET-II, transition region) for different tempering temperatures T_{tmp}

B [T_{tmp}] (mm) [°C]	J_{IC} (N/mm)	K_{JIC} (MPa $m^{0.5}$)
9 [700] $a/W = 0.50$	150	186
3 [700] $a/W = 0.50$	249	240
3 [700] $a/W = 0.25$	264	247
B [T_{tmp}] (mm) [°C]	$DBTT_{USE}$ (°C)	$DBTT_{JID}$ (°C)
10 [600/700]	+45/+10	+93/+65
3 [600/700]	−4/−34	+46/+25

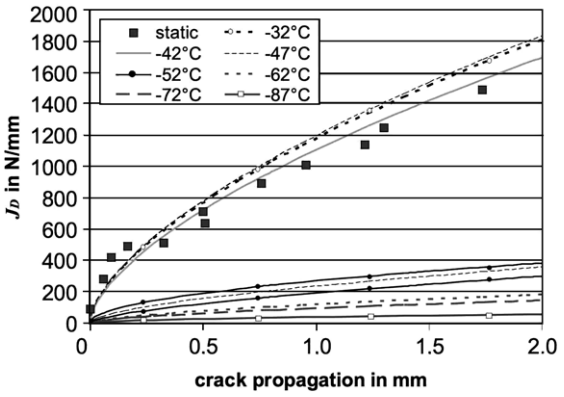

Fig. 3. Determination of J_{ID} (EUROFER 97).

Dynamic J–Δa curves have the same shapes as the curves obtained from static experiments (Fig. 3). The transition of ductile (upper curves) to brittle behaviour (lower curves) occurs suddenly in 3 mm wide plane EUROFER 97 specimens at approximately -44 °C (side-grooved specimen −12 °C) while $DBTT_{USE}$ is at −86 °C.

The fracture-mechanics DBTT is always superior to the Charpy test DBTT. For all specimen types and materials examined, a constant difference of 40–50 °C was found, with the specimen width, B, kept constant:

$$DBTT_{JID} = DBTT_{USE} + \Delta T;$$
$$\Delta T = 40 - 50\,^{\circ}C \text{ for } B = \text{const.} \quad (3)$$

3. Results for irradiated specimens

The evaluation of samples of MANET-I, irradiated to 0.8 dpa at 250–450 °C, provides reproducible values of J. Fracture toughness in the upper shelf is reduced by up to 60% by irradiation, and the DBTT is increased by up to 140 °C. The decrease in fracture toughness depends on the irradiation temperature, being most pronounced at temperatures below 350 °C (Fig. 4 and Table 5).

The strong dependence on the irradiation temperature for the upper shelf as well as the DBTT is similar to the Charpy tests. Comparison of the transition temperatures of both types of tests confirms the relation established above.

4. Conclusion

For the investigated materials, the subsized specimen furnishes conservative results in comparison to the full-size specimens, if the shift in ductile-to-brittle transition is respected, and if the crack opening displacement is determined directly. Geometric modification of the fracture zone, and an appropriate test technique, allow valid results to be obtained, despite specimen dimensions being far below standard recommendations and a/W is lower than 0.5. Fracture-mechanics results under irradiated and unirradiated conditions are presented.

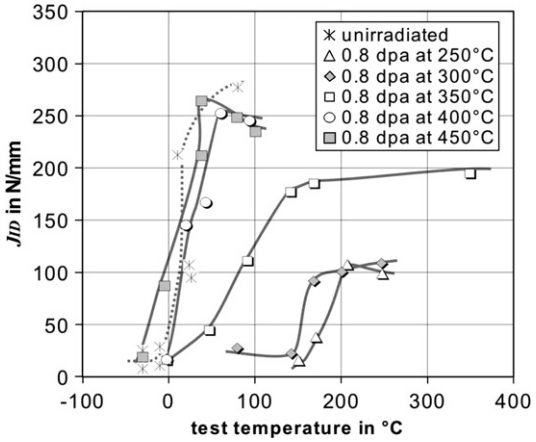

Fig. 4. Determination of J_{ID} in irradiated specimens (MANET-I).

Table 5
Determination of J_{ID} (MANET-I, irradiated)

T_{irr}/dose (°C/dpa)	$J_{ID\ max}$ (N/mm)	$DBTT_{JID}$ (°C)
–/0	277	39
250/0.8	107	178
300/0.8	109	153
350/0.8	185	77
400/0.8	252	16
450/0.8	264	8

References

[1] G.R. Odette, M.Y. He, D. Gragg, D. Klingensmith, G.E. Lucas, J. Nucl. Mater. 307–311 (2) (2002) 1624.
[2] K. Wallin, A. Laukkanen, S. Tähtinnen, ASTM STP 1418 (2002).
[3] M. Nevalainen, R.H. Dodds, Int. J. Fracture 74 (1995) 131.
[4] H.J. Schindler, Matw. u. Werkstofftechnik 32 (6) (2001) 544.
[5] X.P. Zhang, Y.W. Shi, Int. J. Pres. Ves. Pip. 65 (1996) 187.
[6] R. Kaspar, H. Faul, Materialprüfung 43 (1–2) (2001) 18.
[7] H.-C. Schneider, Entwicklung einer miniaturisierten bruchmechanischen Probe für Nachbestrahlungsuntersuchungen, Scientific Report, Forschungszentrum Karlsruhe, FZKA 6605, September 2005.